Chimera State in Structured Heterogeneous Networks

Bo Li
Department of Physics, The Hong Kong University of Science and Technology, Hong Kong

David Saad
Non-linear and Complexity Research Group, Aston University, Birmingham B4 7ET, United Kingdom

(Dated: November 3, 2016)

Chimera states are manifested through the coexistence of synchronous and asynchronous dynamics and have been observed in various systems. To analyze the role of network topology in giving rise to chimera states we study a heterogeneous network model comprising two group of nodes, of high and low degrees of connectivity. The architecture facilitates the analysis of the system, which separates into a densely-connected coherent group of nodes, perturbed by their sparsely-connected drifting neighbors. It describes a synchronous behavior of the densely-connected group and scaling properties of the induced perturbations.

arXiv:1611.00657v1 [nlin.PS] 2 Nov 2016

I. INTRODUCTION

The dynamics of coupled oscillators has been widely studied to understand the synchronization behaviors in complex systems [1–3]. Among the fascinating phenomena observed in these systems the chimera states, which exhibit a coexistence of synchronous and asynchronous domains, have attracted particular interest recently [4]. It came as a surprise that the symmetry-breaking chimera states were observed in symmetric and homogeneous media [5–7]. This phenomena is also reminiscent of the coexistence of equilibrium-like domains in non-equilibrium systems [8].

The analysis of chimera states is generally difficult, due to the heterogeneous interactions between a large number of variables, and appropriate approximations are required. One of the approximations is based on mapping the system onto a low dimensional manifold [9], which facilitates a simplification that leads to tractable solutions. Such approaches are either based on the continuous self consistent mean field theory or rely on the assumption of Ott-Antonsen reduction to simplify the problem [5, 10]. Carefully chosen initial conditions are also necessary to produce chimera states in these symmetric systems. Other studies that do not rely on the system's symmetry [11] have been employed to investigate sinusoidally coupled oscillators in complex networks, which exhibit chimera state behavior from arbitrary initial conditions.

An interesting observation from studies in scale free networks is that nodes of high degrees are more likely to synchronize than nodes of low degrees. This is an example where heterogeneity in network topology results in disparate behaviors across the system [12–14]. Also in models with chaotic oscillators, it was shown that hubs synchronize while low-degree nodes do not [12, 15]. In general, the strong interactions highly-connected oscillatory nodes have with their neighbors distinguishes them from the non-synchronizing low-degree nodes [11]. However, the complex structure of heterogeneous networks, such as scale free or small world networks is not amenable to analysis due to the combined complexity of the network topology and , intractability of the large scale-dynamical model. In this work, we investigate a simple heterogeneous network architecture which supports an easy-to-reach chimera state but is amenable to analysis. It exposes the synchronized equilibrium-like behavior of the densely-connected components and facilitate the derivation of perturbation originated by the sparsely-connected components; finite-size scaling of these perturbation and the corresponding order parameter is also be derived, shedding light on the interplay between the two types of nodes.

II. THE MODEL

We consider a heterogeneous network with degree distribution of two peaks, i.e., the network comprises two classes of nodes, one of which has extensive connectivity scaled with system size N while the nodes in the other has finite connectivity. Denote the two classes as the dense group $\mathcal{D}$ and the sparse group $\mathcal{S}$ respectively. By assigning a large number of intra-group connections between constituents of the dense group $\mathcal{D}$, each node inside $\mathcal{D}$ can receive large number of coordinated signals from within the group, dominating the fluctuations of other neighboring nodes, potentially leading to coherent intra-group dynamics. Conversely, the nodes in the sparse group can be easily perturbed by fluctuation induced by any of its neighbors due to their limited connectivity.

Specifically, to simplify the construction, each node $i \in \mathcal{D}$ is connected to $d_{\mathcal{D}}(\propto N)$ other nodes randomly chosen from the same class $\mathcal{D}$, and each node $j \in \mathcal{S}$ is connected to $d_{\mathcal{S}}(\sim O(1))$ other nodes randomly chosen from the whole system. Let $n_{\mathcal{D}}$ and $n_{\mathcal{S}}$ denote the number of nodes in the dense and sparse groups, respectively. For simplicity, we consider the special case where node $i \in \mathcal{D}$ is connected to all the rest members of $\mathcal{D}$ so that the dense group forms a complete subgraph, and both groups include the same number of nodes, i.e., $d_{\mathcal{D}} = n_{\mathcal{D}} - 1$ and $n_{\mathcal{D}} = n_{\mathcal{S}} = N/2$. Figure 1 is an instance of the proposed

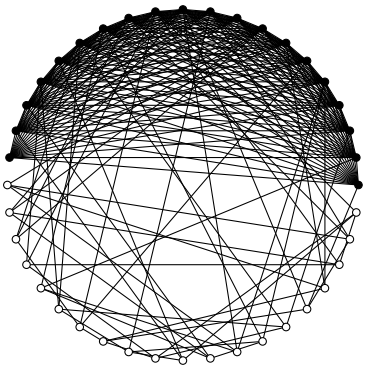

Figure 1. An instance of the heterogeneous network composed of a densely connected (black nodes) and sparsely connected groups (white nodes), where $N = 40$, $d_{\mathcal{S}} = 4$.

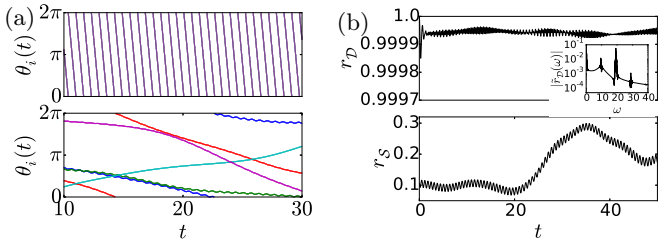

Figure 2. (Color online) (a) Dynamical process of 5 densely (top) and 5 sparsely connected variables (bottom) in a network of size $N = 200$, where the sparse degree is $d_{\mathcal{S}} = 6$, coefficient $K = 10$, and phase $\alpha = \frac{\pi}{2} - 0.2$. In this case, $\Omega = -K(n_{\mathcal{D}}-1)/n_{\mathcal{D}} \sin(\alpha) \approx 9.7$. (b) Evolution of the global order parameters for the densely (top) and sparsely connected variables (bottom). Inset: Power spectrum of $r_{\mathcal{D}}(t)$, which has its main peak at $\omega = 2\Omega$.

network structure with $N = 40$ and $d_{\mathcal{S}} = 4$.

The governing dynamics we consider is the Kuramoto model with phase lag in the chimera state studies [5, 6, 9]

$$\begin{aligned}\dot{\theta}_i &= \omega + \frac{K}{n_{\mathcal{D}}} \sum_{j\in\partial i} \sin(\theta_j - \theta_i - \alpha) \\ &= \omega + \frac{K}{n_{\mathcal{D}}} \sum_{j\in\partial i\cap\mathcal{D}} \sin(\theta_j - \theta_i - \alpha) \\ &\quad + \frac{K}{n_{\mathcal{D}}} \sum_{j\in\partial i\cap\mathcal{S}} \sin(\theta_j - \theta_i - \alpha), \end{aligned} \tag{1}$$

where ∂i stands for the set of nodes adjacent to node i where we have isolated the contribution from the dense and sparse members. Any node $i \in \mathcal{D}$ experiences the global mean field induced by the whole dense group $r_{\mathcal{D}} e^{i\psi_{\mathcal{D}}} := 1/n_{\mathcal{D}} \sum_{j\in\mathcal{D}} e^{i\theta_j}$ and the local field of its sparse neighbors $\rho_i e^{i\varphi_i} := \sum_{j\in\partial i\cap\mathcal{S}} e^{i\theta_j}$, both terms are of order 1,

$$\begin{aligned}\dot{\theta}_i &= \omega + \frac{K}{n_{\mathcal{D}}} \sin\alpha + K r_{\mathcal{D}} \sin(\psi_{\mathcal{D}} \sin(\psi_{\mathcal{D}} - \theta_i - \alpha) \\ &\quad + \frac{K}{n_{\mathcal{D}}} \rho_i \sin(\varphi_i - \theta_i - \alpha). \end{aligned} \tag{2}$$

By construction, the dense group itself forms a $d_{\mathcal{D}}$ regular subgraph, which can reach perfect phase synchronization if the contribution from the sparse neighbors are negligible [16], i.e., $\theta_i = \Omega t + const$, $\Omega = \omega - K(n_{\mathcal{D}} - 1)/n_{\mathcal{D}} \sin(\alpha)$, for all $i \in \mathcal{D}$. This will hold true in the thermodynamic limit $n_{\mathcal{D}} \to \infty$; in which case the densely-connected group $\mathcal{D}$ on its own exhibits an equilibrium-like behavior within the global non-equilibrium system [8]. In finite systems, the effect of sparse neighbors can be regarded as a finite size perturbation with strength of order $1/n_{\mathcal{D}}$ on the coherent dynamics of the densely-connected members $\theta_i(t) = \Omega t + \varepsilon_i(t)$.

The argument cannot be applied to the sparse group. Firstly, we notice that for node $j \in \mathcal{S}$, $|\dot{\theta}_j| \leq \omega + Kd_{\mathcal{S}}/n_{\mathcal{D}} \ll \Omega$, thus it does not follow the coherent dynamics of the densely-connected group and global synchronization of the whole system is not attainable. Secondly, the irregularity of the sparse subgraph and presence of phase lag interfere with phase synchronization. Finally, sparse variables are easily disturbed by noisy signals from their neighbors due to their finite connectivity. We define the global order parameter of the sparse group $r_{\mathcal{S}} := \left|1/n_{\mathcal{S}} \sum_{i\in\mathcal{S}} e^{i\theta_i}\right|$ measuring their incoherence.

III. ANALYSIS AND RESULTS

Without loss of generality, let $\omega = 0$ in the following discussion. In Fig. 2, we demonstrate the dynamics of a network with $N = 200$ and $d_{\mathcal{S}} = 6$ governed by Eq. (1). The dense variables dynamics is coherent with a high phase velocity exhibiting minor deviations from each other, revealed by the small deviation of $r_{\mathcal{D}}(t)$ from 1, shown in Fig. 2(b). On the other hand, the sparse variables are drifting slowly and incoherently. The observed partial synchronization phenomenon constitutes a chimera state. Interestingly, the chimera state is easily obtained in the proposed topology by starting with arbitrary initial conditions, as shown in Fig. 3. This is similar to what has been observed in [11].

In the following, we analyze the deviation of the densely-connected variables from perfect synchronization due to the interaction with the sparsely-connected group. Expanding the phase of a dense group variable i with respect to small perturbation ε_i such that $\theta_i(t) = \Omega t + \varepsilon_i(t)$, and defining $g(\varepsilon) = 1 - r_{\mathcal{D}}(t)$, $f(\varepsilon) = \psi_{\mathcal{D}}(t) - \Omega t$ one obtains

$$\begin{aligned} r_{\mathcal{D}} e^{i\psi_{\mathcal{D}}} &= e^{i\Omega t} \frac{1}{n_{\mathcal{D}}} \sum_{i\in\mathcal{D}} e^{i\varepsilon_i} \\ &= e^{i\Omega t} \left[1 + \frac{i}{n_{\mathcal{D}}} \sum_{i\in\mathcal{D}} \varepsilon_i - \frac{1}{2n_{\mathcal{D}}} \sum_{i\in\mathcal{D}} \varepsilon_i^2 + O(\varepsilon^3)\right], \end{aligned}$$

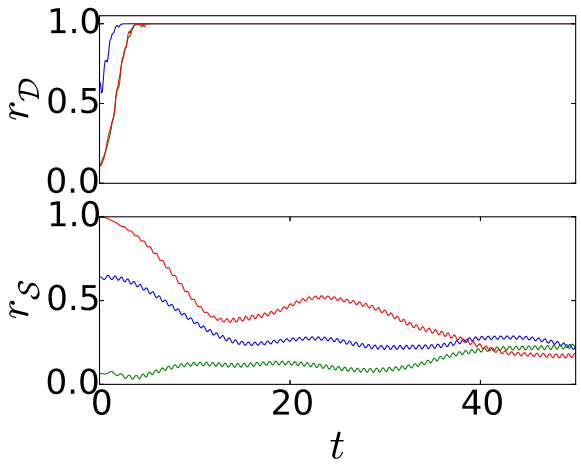

Figure 3. (Color online) Evolution of the global order parameters for the dense (top) and sparse (bottom) groups, starting from different initial conditions. Blue: the initial phases of all variables are drawn from the uniform distribution ranging from 0 to π. Green: the initial phases of all variables are drawn from the uniform distribution ranging from 0 to 2π. Red: the initial phases of all dense variables are drawn from the uniform distribution ranging from 0 to 2π, while that of sparse variables share the same phase value.

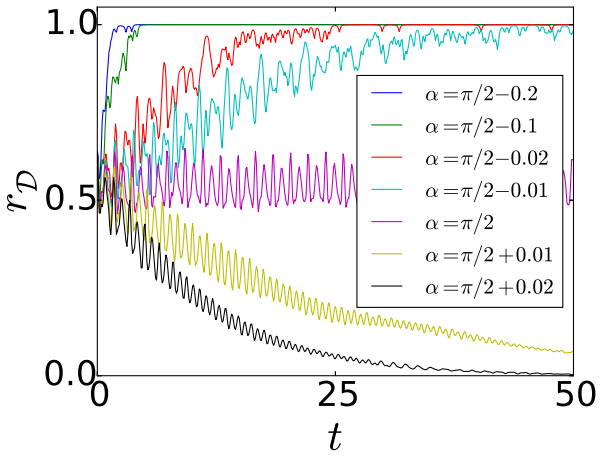

Figure 4. (Color online) Evolution of $r_{\mathcal{D}}$ for different phase lags α and a network with $N = 200$ variables, sparse degree $d_{\mathcal{S}} = 6$ and coefficient $K = 10$.

from results in leading order in ϵ^2,

$$g(\varepsilon) \approx \frac{1}{2n_{\mathcal{D}}} \sum_{i\in\mathcal{D}} \varepsilon_i^2 - \frac{1}{2n_{\mathcal{D}}^2} \left(\sum_{i\in\mathcal{D}} \varepsilon_i \right)^2, \tag{3}$$

$$f(\varepsilon) \approx \frac{1}{n_{\mathcal{D}}} \sum_{i\in\mathcal{D}} \varepsilon_i. \tag{4}$$

Assuming ε_i, and subsequently $g(\varepsilon)$ and $f(\varepsilon)$ are small, then Eq. (2) can be expressed as

$$\begin{aligned}
\dot{\varepsilon}_i &= K \sin\alpha + K\,(1-g(\varepsilon)) \sin\left(f(\varepsilon) - \varepsilon_i - \alpha\right) \\
&\quad + \frac{K}{n_{\mathcal{D}}} \rho_i \sin(\varphi_i - \Omega t - \varepsilon_i - \alpha) \\
&\approx (K\cos\alpha)\left[f(\varepsilon) - \varepsilon_i\right] - \left[K\,\partial_{\varepsilon_i} g(\varepsilon)|_{\varepsilon_i=0} \sin\alpha\right] \varepsilon_i \\
&\quad + \frac{K}{n_{\mathcal{D}}} \rho_i \sin(\varphi_i - \Omega t - \alpha) \\
&\quad - \frac{K}{n_{\mathcal{D}}} \rho_i \cos(\varphi_i - \Omega t - \alpha)\varepsilon_i,
\end{aligned} \tag{5}$$

where only first order terms in ε_i are retained. Furthermore, in the large size limit $1/n_{\mathcal{D}}$ is considered to be small and the last term of Eq. (5) can be ignored since it contains the product of two small quantities, ε_i and $1/n_{\mathcal{D}}$. Assuming the fluctuations ε_i are uncorrelated across sites, $f(\varepsilon) = 1/n_{\mathcal{D}} \sum_{i\in\mathcal{D}} \varepsilon_i$ smooths out the fluctuations of individual variables and becomes smaller compared to any single fluctuations ε_i; it is therefore omitted in the following. Additionally, to leading order we have $\partial_{\varepsilon_i} g(\varepsilon)|_{\varepsilon_i=0} = -1/n_{\mathcal{D}}^2 \sum_{j\neq i} \varepsilon_j$, which vanishes for large $n_{\mathcal{D}}$, such that the corresponding term in Eq. (5) can be omitted for fixed $\alpha < \pi/2$, leading to

$$\dot{\varepsilon}_i = -(K\cos\alpha)\varepsilon_i + \frac{K}{n_{\mathcal{D}}} \rho_i \sin(\varphi_i - \Omega t - \alpha). \tag{6}$$

By definition of the local mean field of ρ_i and φ_i, the last term of Eq. (6) can be expressed as

$$\frac{K}{n_{\mathcal{D}}} \rho_i \sin(\varphi_i - \Omega t - \alpha) = \frac{K}{n_{\mathcal{D}}} \sum_{j\in\partial i\cap\mathcal{S}} \sin(\theta_j - \Omega t - \alpha).$$

Since the phase velocity $|\dot{\theta}_j| (\leq K d_{\mathcal{S}}/n_{\mathcal{D}})$ of the sparsely-connected variables j is much smaller than the oscillation of Ωt, as shown in Fig. 2(a), the two time scales within the sin function can be separated, allowing one to view ρ_i and φ_i as quench variables within a time frame of a few periods. As $\Omega = -K(n_{\mathcal{D}}-1)/n_{\mathcal{D}} \sin(\alpha) \approx -K\sin(\alpha)$ for large $n_{\mathcal{D}}$, Eq. (6) can be integrated o provide

$$\varepsilon_i(t) = c_1 e^{-(K\cos\alpha)t} + \frac{1}{n_{\mathcal{D}}} \rho_i \sin(\varphi_i - \Omega t - 2\alpha). \tag{7}$$

This solution Eq. (7) has a decay term of rate $K\cos(\alpha)$ and a stationary oscillatory term of frequency $\Omega = -K\sin(\alpha)$. The stationary part of ε_i scales as $1/n_{\mathcal{D}}$, which is consistent with the derivation that treats both ε_i and $1/n_{\mathcal{D}}$ as small quantities at the same time. We can therefore deduce that the dense group converges faster to the steady solution for smaller α values, where $\alpha = \pi/2$ signals the onset of instability of the chimera state, as shown in Fig 4.

The deviation $\varepsilon_i(t)$ has an oscillatory behavior of frequency Ω. From Eq. (3), we expect that $r_{\mathcal{D}}(t) = 1 - g(\varepsilon)$ oscillates primarily at a frequency 2Ω, which is verified by the power spectrum of $r_{\mathcal{D}}(t)$ from the numerical experiment in the inset of Fig. 2(b).

In the steady state, substituting the solution of $\varepsilon_i(t) = \rho_i/n_{\mathcal{D}} \sin(\varphi_i - \Omega t - 2\alpha)$ into Eq. (3), one obtains an

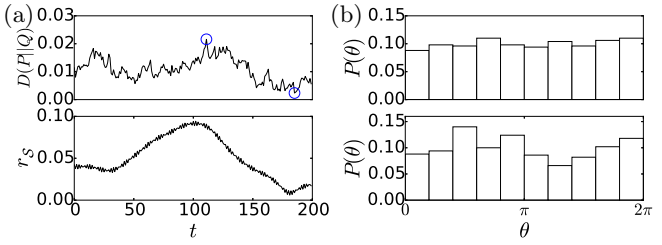

Figure 5. (Color online) (a) Top: Kullback–Leibler (KL) divergence between the phase distribution $P(\theta_j)$ of the sparse variables and the uniform distribution $Q(\theta_j) = const$, defined as $D(P||Q) := \sum_x P(x)\ln(P(x)/Q(x))$. The parameters of the network are $N = 1000$, $d_S = 6$, $\alpha = \pi/2 - 0.2$. $P(\theta_j)$ is approximated by a histogram with 10 bins, in which case the upper bound for the KL divergence is $\max_P D(P||Q) = \ln 10 \approx 2.30$. The observed small KL divergence $D(P||Q)$ implies that the phase distribution is close to uniform. Bottom: The global order parameter r_S for the sparse group exhibits small values; $r_S = 0$ when the phases are uniformly distributed. (b) The distribution $P(\theta_j)$ at the points with the lowest (upper panel) and highest (lower panel) KL divergence in the observed time window, as marked by the two blue circles in the upper panel of (a).

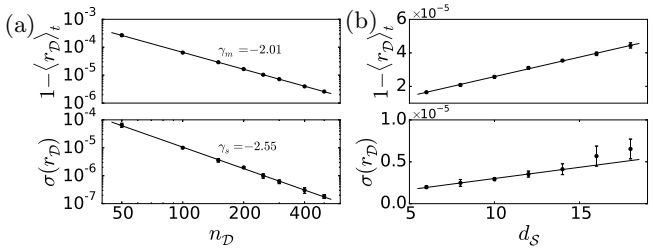

Figure 6. (a) Mean and variance of r_D for an observed time window as a function of n_D with fixed $d_S = 6$. The data follows the scaling of the form $(1 - \langle r_D\rangle_t) \sim n_D^{\gamma_m}$, $\sigma(r_D) \sim n_D^{\gamma_s}$, with coefficients $\gamma_m = -2.01$, $\gamma_s = -2.55$. Each data point is averaged over 10 realizations. (b) The values $1-\langle r_D\rangle_t$ and $\sigma(r_D)$ as a function of the sparse degree connectivity d_S with fixed $n_D = 200$; both increase linearly with d_S. Each data point is average over 10 realizations. In the lower panel, the straight line is fitted to the first five data points, while the measurement of the last two points are rather imprecise and one expects the linear dependence to gradually break down as the ratio d_S/d_D increases.

expression for $g(\varepsilon)$, and consequently for r_D. It is observed that the distribution of sparsely-connected variables phases is close to uniform, as illustrated in Fig. 5. Thus we compute the time average r_D by averaging over the phase angles of the sparse variables, where phases are assumed to be independently and uniformly distributed in $[0, 2\pi)$, i.e., $P(\theta_j) = 1/2\pi$, $\forall j \in \mathcal{S}$. It is sufficient to consider a single instance of $\varepsilon_i(t)$

$$\epsilon_i = \frac{\rho_i}{n_D}\sin(\varphi_i) = \frac{1}{n_D}\sum_{j\in\partial i\cap\mathcal{S}}\sin(\theta_j).$$

Since $\mathbb{E}[\sin(\theta_j)] = 0, \mathbb{E}[\sin^2(\theta_j)] = 1/2, \mathbb{E}[\sin^4(\theta_j)] = 3/8$, it is straightforward to obtain the mean and variance of r_D,

$$\begin{aligned}\mathbb{E}[r_D] &= \mathbb{E}\left[1 - g(\epsilon)\right] \\ &= 1 - \frac{1}{2n_D}\mathbb{E}\left[\sum_{i\in D}\epsilon_i^2\right] + \frac{1}{2n_D^2}\mathbb{E}\left[\left(\sum_{i\in D}\epsilon_i\right)^2\right] \quad (8)\\ &= 1 - \frac{d_S}{8n_D^2} + \frac{d_S^2}{16n_D^3}, \quad (9)\end{aligned}$$

$$\begin{aligned}\mathbb{E}[r_D^2] - \mathbb{E}[r_D]^2 &= \mathbb{E}\left[\left(1-g(\epsilon)\right)^2\right] - \mathbb{E}[1-g(\epsilon)]^2 \\ &= \frac{1}{32n_D^5}\left(d_S^2 - \frac{3}{2}d_S\right) + O\left(\frac{1}{n_D^6}\right) \quad (10)\end{aligned}$$

Therefore, to leading order, the mean of $1 - \mathbb{E}[r_D]$ scales as d_S/n_D^2, while the standard deviation $\sigma(r_D)$ scales as $d_S/n_D^{2.5}$. The finite size scaling behavior is confirmed, in full agreement, by numerical simulations as shown in Fig. 6.

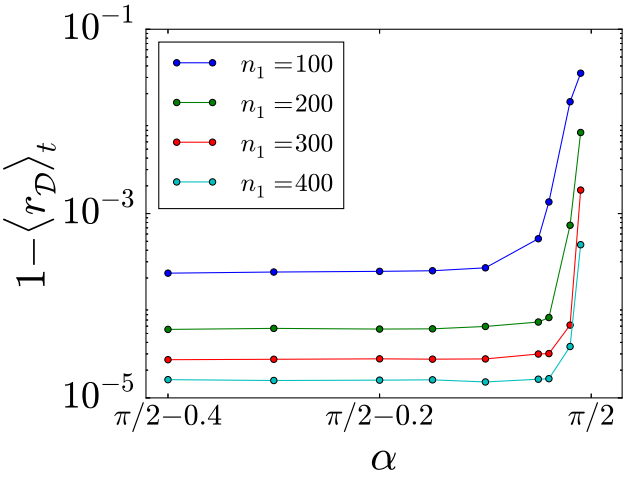

Figure 7. Expected first order corrections $1 - \langle r_D\rangle_t$ vs α for different system sizes, measured at the stationary states.

The obtained solution of r_D in Eq. (9) is independent of α. Nevertheless, we remark that the derivation breaks down when α is close to $\pi/2$, in particular for $\alpha \sim \tan^{-1}(n_D^2)$, where the term $\left[K\,\partial_{\varepsilon_i} g(\varepsilon)|_{\varepsilon_i=0}\sin\alpha\right]\varepsilon_i$ starts to dominate $(K\cos\alpha)\varepsilon_i$ in Eq. (5). We can see this effect in Fig. 7 where for a wide range of α values away from $\pi/2$, the deviation to perfect synchronization in the stationary state is independent of α. When α gets closer to $\pi/2$, the deviation starts to increase; the onset of this deviation occurs later for larger systems, as expected.

IV. CONCLUSION

We study a simple heterogeneous network architecture that supports easy-to-reach chimera states and is

amenable to analysis. The network comprises two interconnected components of densely connected and sparsely connected variables. The heterogeneity separates the time scales of the dynamics of the two components, leading to disparate behaviors of the two groups. We showed that the densely connected group maintains a synchronized and coherent dynamics, while the dynamics of sparse group variables is incoherent. Furthermore, we derived a self-consistent mean field theory for these networks, by viewing the contribution of the sparse variables as $1/n_{\mathcal{D}}$-scale perturbations to the dense group's dynamics. Using this framework we obtained expressions for the dense group order parameter that exhibits perfect synchronization, and subsequently its dependence on phase lag parameter, network size and network connectivity. The model facilitates the analysis of large systems comprising interacting oscillatory variables to provide new insight and understanding of their complex dynamical behaviors. We envisage that this and similar models could be employed to explore the properties of other heterogeneous network architectures.

ACKNOWLEDGEMENT

Support from the Overseas Research Awards of Hong Kong University of Science and Technology (BL) and The Leverhulme Trust grant RPG-2013-48 (DS) is acknowledged. The work was carried out during an extended visit to Aston University, Bo Li would like to thank Aston for the hospitality.

[1] Juan A. Acebrón, L. L. Bonilla, Conrad J. Pérez Vicente, Félix Ritort, and Renato Spigler. The Kuramoto model: A simple paradigm for synchronization phenomena. *Rev. Mod. Phys.*, 77:137–185, Apr 2005.

[2] S. Boccaletti, J. Kurths, G. Osipov, D.L. Valladares, and C.S. Zhou. The synchronization of chaotic systems. *Physics Reports*, 366(1-2):1 – 101, 2002.

[3] Francisco A. Rodrigues, Thomas K. DM. Peron, Peng Ji, and Jürgen Kurths. The Kuramoto model in complex networks. *Physics Reports*, 610:1 – 98, 2016.

[4] Mark J Panaggio and Daniel M Abrams. Chimera states: coexistence of coherence and incoherence in networks of coupled oscillators. *Nonlinearity*, 28(3):R67, 2015.

[5] Kuramoto Y. and Battogtokh D. Coexistence of coherence and incoherence in nonlocally coupled phase oscillators. *Nonlinear Phenomena In Complex Systems*, 5(4):380–385, 2002.

[6] Shin-ichiro Shima and Yoshiki Kuramoto. Rotating spiral waves with phase-randomized core in nonlocally coupled oscillators. *Phys. Rev. E*, 69:036213, Mar 2004.

[7] Daniel M. Abrams and Steven H. Strogatz. Chimera states for coupled oscillators. *Phys. Rev. Lett.*, 93:174102, Oct 2004.

[8] David Saad and Alexander Mozeika. Emergence of equilibriumlike domains within nonequilibrium ising spin systems. *Phys. Rev. E*, 87:032131, Mar 2013.

[9] Daniel M. Abrams, Rennie Mirollo, Steven H. Strogatz, and Daniel A. Wiley. Solvable model for chimera states of coupled oscillators. *Phys. Rev. Lett.*, 101:084103, Aug 2008.

[10] Edward Ott and Thomas M. Antonsen. Low dimensional behavior of large systems of globally coupled oscillators. *Chaos*, 18(3), 2008.

[11] Yun Zhu, Zhigang Zheng, and Junzhong Yang. Chimera states on complex networks. *Phys. Rev. E*, 89:022914, Feb 2014.

[12] Changsong Zhou and Jürgen Kurths. Hierarchical synchronization in complex networks with heterogeneous degrees. *Chaos*, 16(1), 2006.

[13] Jesús Gómez-Gardeñes, Yamir Moreno, and Alex Arenas. Paths to synchronization on complex networks. *Phys. Rev. Lett.*, 98:034101, Jan 2007.

[14] Jesús Gómez-Gardeñes, Sergio Gómez, Alex Arenas, and Yamir Moreno. Explosive synchronization transitions in scale-free networks. *Phys. Rev. Lett.*, 106:128701, Mar 2011.

[15] Tiago Pereira. Hub synchronization in scale-free networks. *Phys. Rev. E*, 82:036201, Sep 2010.

[16] Per Sebastian Skardal, Dane Taylor, Jie Sun, and Alex Arenas. Erosion of synchronization in networks of coupled oscillators. *Phys. Rev. E*, 91:010802, Jan 2015.